CHARACTERIZATION OF THE FLOW FIELD THROUGH A STAGGERED DISTRIBUTION OF CYLINDERS

Valentina Cavedon, Maurizio Righetti & Aronne Armanini

Department of Civil and Environmental Engineering, University of Trento, Italy

E-mails: valentina.cavedon@ing.unitn.it,
maurizio.righetti@ing.unitn.it,
aronne.armanini@ing.unitn.it

Abstract

In the paper some laboratory results on the flow field through rigid unsubmerged vegetation are presented and discussed. Vegetation is modeled using rigid, emergent, cylinders in a laboratory channel, uniformly distributed in staggered configuration. The turbulent structure of the flow field is characterized by means of the Particle Image Velocimetry (PIV) technique. Measurements are carried out at 12 different vertical light sheets at different transversal positions and the data are analyzed both in time and in space, according with the double-averaging methodology. The measurements of the velocity field allow one to compare the averaged velocity of the flow with the local velocity, with particular attention to the bed region, in order to relate it with the sediment entrainment. The experimental data show that the flow field is highly heterogeneous in space: zones of wakes alternate with boundary layer-like zones, quasi-log velocity profiles zones and jet-like zones. The distribution of velocities and its influence on the transport phenomena are discussed in the paper.

Introduction

Turbulence production and transport phenomena can have several sources in natural rivers. When rivers with rigid vegetation are concerned, the generation of wakes around stems and bed shear are the phenomena that mainly affect the turbulent flow field. The fluid-vegetation interaction, which generates different kinds of instabilities, such as wake generation and horseshoe vortex, together with the bed effect (including both grain roughness and bed forms instabilities) concur to generate a turbulent flow which is hard to define as "uniform". The characteristics of the resulting flow depend on the distribution of stems, nature and geometry of bed forms, besides the obvious dependence on flow depth.

The analysis of turbulence structure through vegetation is particularly important also because the dynamics of the flow and the drag coefficient - both due to vegetation and bed roughness - are strictly related. Moreover, the drag coefficient of stems in a colony is influenced by the interactions between relative stems and mutual interactions between cylinders and wakes. Some papers tried to distinguish the behavior of drag depending on the distance between elements (Ishikawa, Mizuhara, and Ashida 2000b; Kothyari, Hashimoto, and Hayashi 2009; Li and Shen 1973; Tanino and Nepf 2008) and consequently in which way the mutual interaction between cylinders develops and how it can be taken into account. It is generally accepted that these interactions can play a crucial role also in the sediment entrainment and transport.

In case of presence of vegetation, the formulation of the vertical distribution of velocity or of the law of resistance can be totally different by what given by a boundary layer approach. In flows with strong spatial variation, such as in the present case, the application of the Double-Averaged Methodology (called also simply DAM) can be useful. During the last 30 years, this method has been developed by many authors and applied to different kinds of environmental flows (see e.g. Finnigan (2000) and Nikora (2010)) which present strong spatial variation in motion. *Double-average* means that the velocity, defined for each point of a control volume of a fluid in motion, is first averaged in the space (spatial average), and then the spatial average is averaged in the time, or viceversa.

Double-averaged equation through vegetation is the most used and useful method to evaluate the characteristic velocities of flow. Many authors have expressed dif-

ferent double-averaged equations by using different work hypotheses (Whitaker 1999), which express different formulations of the DA equations. Double-averaged equations can be useful because they allow to divide the spatially homogeneous part to the deviations in space of the flow. The spatial variations are summarized in the dispersive components of the DA equations.

Theoretical approach

In the double-average method, every term of the fluid equations for each point of the domain of analysis can be broken down into three terms:

$$u(t) = \bar{u}(t) + \tilde{u}(t) + u'(t) \tag{1}$$

in which the spatial average $\langle u(t) \rangle$ is already expressed into the two terms: $\langle u(t) \rangle = \bar{u}(t) + \tilde{u}(t)$, where $\bar{u}(t)$ is the time-averaged velocity and $\tilde{u}(t)$ the fluctuating part.

By using the variables in equation (1), the double-averaged equations can be obtained. In particular they can be evaluated with two different methodologies:

1. by applying the spatial average to the Reynolds equations, which are already temporal averaged;
2. by applying the spatial average to the Navier-Stokes equations and then the ensemble average to the resulting equations.

Several authors (e.g. Nikora et al. (2007)) sustain that the first method seems the most suitable for the fluid mechanics topics, especially because it follows the classical approach and results are clearest for hydraulic scientists.

The simplest equations, that are reported only as example, and that are used by several authors, among them Righetti (2008) and Righetti and Armanini (2002), are obtained neglecting the viscous contributions on averages in horizontal layer. The resulting equations are:

$$\begin{cases} g i_b - \langle \dfrac{\partial \tilde{p}}{\partial x} \rangle - \frac{1}{\phi} \dfrac{\partial \phi \langle \tilde{u}\tilde{w} \rangle}{\partial z} - \frac{1}{\phi} \dfrac{\partial \phi \langle u'w' \rangle}{\partial z} = 0 \\ g + \dfrac{1}{\rho} \dfrac{\partial \langle \bar{p} \rangle}{\partial z} + \frac{1}{\rho} \langle \dfrac{\partial \tilde{p}}{\partial z} \rangle + \dfrac{1}{\phi} \dfrac{\partial \phi \langle \overline{w'^2} \rangle}{\partial z} + \dfrac{1}{\phi} \dfrac{\partial \phi \langle \tilde{w}^2 \rangle}{\partial z} = 0 \end{cases} \tag{2}$$

where u, v and w are the instantaneous components of velocity along the three main directions x, y and z. In equation (2) is present the term ϕ which describes the porosity of vegetation (in the cited approaches, it is referred to submerged and flexible vegetation). Implicitly in equation (2) is also present the definition of the drag coefficient of vegetation, since the variations of pressure in the xy-plane are related with the drag coefficient. Despite that many experimental observations show that the drag coefficient is a function of plant density and arrangement and of flow conditions (see e.g Ishikawa, Mizuhara, and Ashida (2000a); Kothyari, Hashimoto, and Hayashi (2009) and Tanino and Nepf (2008)), usually this term is considered as a constant in many numerical models. This can be a rough approximation which can lead to inaccuracy, especially for low Reynolds number conditions.

In the present work, we will show the spatial heterogeneities of the flow field in vegetated flows and we will analyze it with reference on the entrainment and turbulent transport of bed particles. In particular, we will not analyze the dispersive component of the flow field, but only the time averaged velocities in some representative vertical planes, and the spatial averaged components of the flow field, with the aim to infer the implication for sediment entrainment and transport.

Experimental set up

Generally the study of resistance exerted by rigid stems is approached by modeling the stems with rigid cylinders at constant diameter. The publications which treat the topic with this generalization are numerously. In the paper we describe new experimental data for evaluation of the flow field through cylinders considering a geometrical and constant distribution of cylinders.

The experiments are carried out in a laboratory channel. The channel is $15\ \mathrm{m}$ long, that is sufficient to obtain uniform flow conditions in a sufficiently long reach for the measurements, and $0.5\ \mathrm{m}$ wide. The slope of the channel can be changed and for the Particle Image Velocimetry (PIV) analysis the slope is 0.8%. The lateral walls are of glass ($0.7\ \mathrm{m}$ high); the bottom of the channel is made of rigid plastic material and grains of sand are glued, in order to have a grain roughness. The water discharge is controlled by a gate connected to a pump.

In the laboratory channel, the presence of rigid stems is modeled using cylindrical elements fixed at the bottom of the channel, rigid and always emergent. The distribution of the cylinders is geometrical (*staggered distribution*) and constant along the channel. The distance between two adjacent cylinders is $15\ \mathrm{cm}$, and the diameter of each cylinder is $d_p = 1\ \mathrm{cm}$.

In order to evaluate the velocity field through the cylinders, the PIV technique is used. This experimental method is widely used in fluid dynamics because it gives simultaneous and detailed information on the velocity field in a whole domain of investigation. Neutrally buoyant particles having grain size smaller than $256\ \mu\mathrm{m}$ are used as tracer. The images are taken for very brief time intervals, namely for a very high frequency of acquisition. The averaged velocity of the flow considered for the tests is about $14\ \mathrm{cm/s}$.

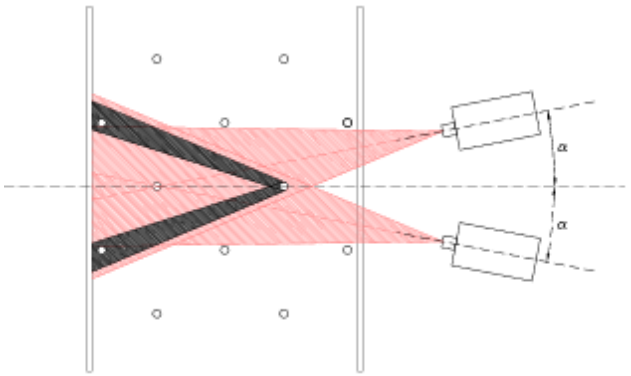

Figure 1: Disposition of cylinder in the laboratory channel and set up of cameras with respect the channel.

Hence, it is chosen to work with the maximum resolution and an acquisition velocity of 250 fps, which is sufficient to evaluate the cross correlation between particles in motion and to have also a good definition in time of the velocity field. The set up of the two high speed cameras (Photron) is sketched in Figure 1: they are located close to the lateral wall and they form an angle between them, which allows to extend the visible field for the cameras, limiting the effect of obscuration due to the presence of cylinders in front of the light plane.

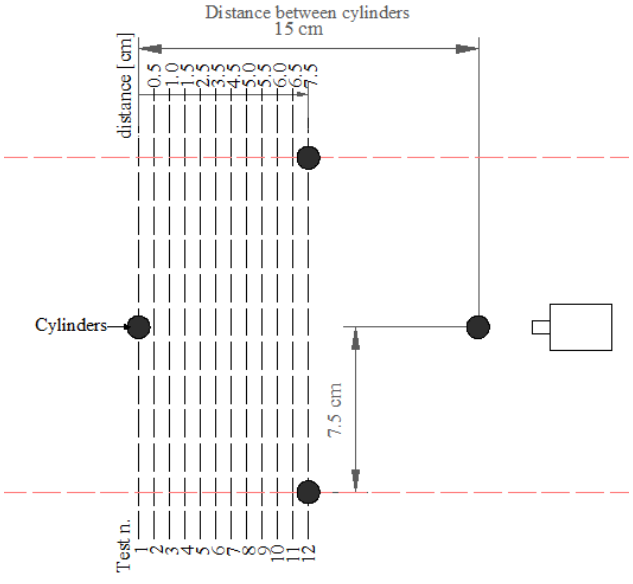

Figure 2: The twelve light sheet used for measuring the whole flow field through cylinders.

First of all, the laser must be arranged in order to have the light sheet perpendicular to the bottom and orientated with the x-axis, coincident with the main flow direction. Thanks to the symmetrical properties of the distribution of cylinders, all the flow field is described with 12 vertical planes (see Figure 2).

The flow is extremely turbulent and hence the free surface is oscillating. In order to avoid the oscillation, which might give problems of reflection of the light, a thin prism in plexiglass is posed in correspondence to the free surface. Clearly the prism affects the region of the flow field closer to the free surface (about $1/5$ of the water depth), which hence will be discarded.

Data analysis

With the instantaneous data of velocity, the time averaged velocity is obtained for each vertical plane in Figure 2.

Data processing has been performed by means of a commercial software (Flow Manager Dantec®) and by means of post-processing routines written in MatLab®. Before of PIV processing, images have been rectified in order to avoid the distortion due to non orthogonal acquisition. The double averaged velocity for the considered control volume is: $\langle \bar{u} \rangle = 0.139$ m/s in the x direction, and $\langle \bar{v} \rangle = 0.0002$ m/s, that is about 0, in the vertical direction. In the following, not all the plane results are reported, but only the most significant cases.

In the Figure 3, the time averaged velocity, $\bar{u}$, is represented for the first plane (test 1, Figure 2) in a dimensionless point of view, i.e. compared with the double-averaged velocity $\bar{u}/\sqrt{\langle \bar{u} \rangle^2 + \langle \bar{v} \rangle^2}$ and $\bar{v}/\sqrt{\langle \bar{u} \rangle^2 + \langle \bar{v} \rangle^2}$. In the same figure, also the isovelocity are represented in gray scale; in the legend of the figure, the symbol U is the module of the double averaged quantities, that is $U = \sqrt{\langle \bar{u} \rangle^2 + \langle \bar{v} \rangle^2}$ and $u = \sqrt{\bar{u}^2 + \bar{v}^2}$. For the evaluation of the above dimensionless quantities, $\langle \bar{v} \rangle^2$ is considered equal to zero. The horizontal axis represents the dimensionless distance between cylinders, x/Λ_p. The vertical direction is represented as z/h, where h is the water depth, and the vertical depth that is considered as valid domain is for $z/h < 0.75$. The rest is generally influences by the prism of plexiglass.

Figure 3 shows the measured flow field for test 1, the vertical plane containing the axis of the cylinder. It is evident that the velocity has a strong decrease going toward the cylinder. In the region immediately downstream the cylinder ($x/\Lambda_p < 0.2$), a zone with negative longitudinal velocity is present, as a result of the recirculation that takes place in the separation zone. Going further downstream, out of the separation zone, the longitudinal velocity assumes positive values. This behavior is more or less present all along the flow depth. In this section, the velocity does never reach the uniformity, and the maximum value is located upstream the cylinder ($u/U = 0.9$), while all the region downstream is strongly affected by its presence. Figure 4 is a detail of the velocity vectors close to the bottom and to the cylinder.

In Figure 5 is plotted the vertical component of veloc-

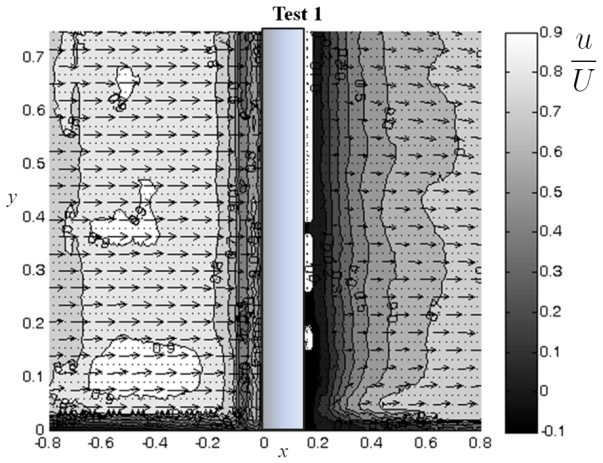

Figure 3: Time averaged velocity for the test 1.

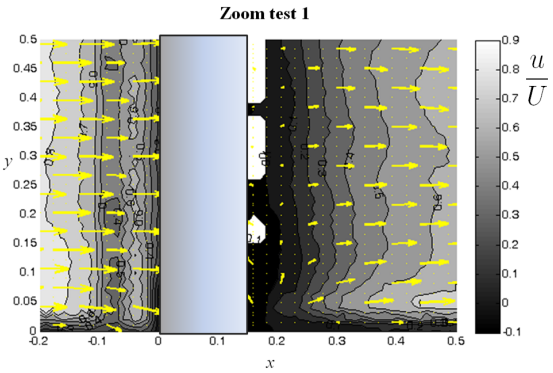

Figure 4: Time averaged velocity for the zoomed test 1.

ity for the plane of test 1 and the differences obtainable by averaging the values of $\bar{v}$ in five different ranges of x/Λ_p. It is particularly interesting (Figures 4 and 5) the tendency of the flow, upstream the cylinder and close to the bottom, to go down toward the bottom itself. This feature of the flow field is well known and deeply discussed (Kirkil, Constantinescu, Ettema, et al. 2008), at least for the case of an isolated cylinder. In that zone the vertical component of the instantaneous velocities is always oriented toward the bed. It is also known that in this region a significant scour is present in case of mobile bed.

Figure 6 shows how the profiles of Reynolds stresses ($\overline{u'w'}/u_*^2$) change, in test 1, from downstream to upstream the cylinder and at different distances. In particular, five different profiles are shown: two averaged profiles of the Reynolds stresses for a range of data far from the cylinder, both downstream and upstream ($-1 < x/\Lambda_p < -0.5$ upstream, and $0.5 < x/\Lambda_p < 1$ downstream); two vertical profiles very close to the cylinder ($x/\Lambda_p = -0.05$ upstream, and $x/\Lambda_p = 0.05$ downstream); the last one is the averaged profile for all the domain ($-1 < x/\Lambda_p < 1$). In all the cases, the Reynolds stresses profiles are very different from the traditional triangular profiles. Therefore, the extension of the effects of a cylinder does not stop before the achievement of a second cylinder, by confirming the mutual interaction between two cylinders. In other words, the recirculating zone which develops downstream a cylinder affects the flow field upstream the following cylinder. Hence, a boundary layer-like flow field cannot develop in the planes in line with the cylinders, like the plane of Test 1 and Test 12 (see Figure 2).

Figure 6 shows that immediately upstream the cylinder, in Test 1 (see Figure 2), the local Reynolds stresses assume negative values but not particularly high in module; here the longitudinal component of the averaged velocity (Figure 5) is very small, due to the formation of a stagnation point on the upstream face of the cylinder. All these consideration allow one to infer that the recirculating region just downstream the cylinder, characterized by evident erosion phenomena, actively participate to the sediment detachment but not to the sediment transport. The erosion processes which take place are particularly significant (See e.g. Ettema, Nakato, and Muste (2008)) but seems to be poorly related to the local values of the Reynolds stresses $u'w'$, therefore in this area the scouring can be hardly be related to a shear mechanism.

The profile closest to the cylinder, represented in Figure 6, confirms what already said for the vertical component of velocity, since upstream the cylinder $\overline{u'w'} > 0$. Positive values of Reynolds stresses means that the shear stress at the bed ($\tau = -\rho\overline{u'w'}$) is directed upstream, and this is due to the transversal axis vortex that takes place at the bottom (Kirkil, Constantinescu, Ettema, et al. 2008). Positive values of the Reynolds stresses mean that, if a shear mechanism takes place just upstream the cylinder, the entrainment of sediment is directed upstream. Moreover the almost negligible values of the longitudinal velocity upstream the cylinder, due to the stagnation point, once more allows one to infer that the downstream convective motion of sediment in this region is negligible.

The same remarks can be done as far as concerns the behavior of the flow downstream the cylinder. The vertical components (Figures 4 and 5) are positive, i.e. directed upward. This corresponds to a decrease of the module of Reynolds stresses close to the cylinder (Figure 6), which however maintains a negative value. It means that there is an area close to the cylinder in which the shear stress is directed upstream and hence it does not actively participate to the sediment transport, but it rather behaves as a sink for sediment. Indeed it can be argued that the entrained sediment particles are "entrapped" in the recirculating zone. In all the region downstream the cylinder and close to the bed, however, the tendency of the Reynolds stresses is to

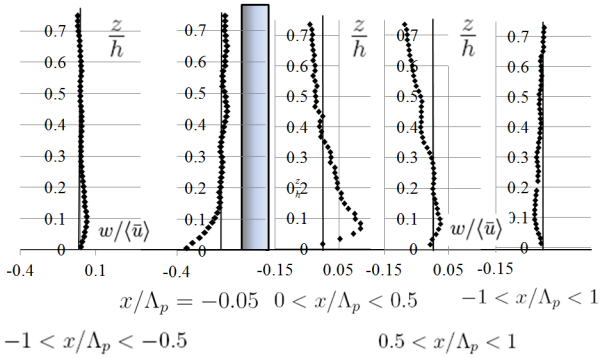

Figure 5: Vertical component of the time and spatial averaged velocity of test 1. In the figure, five profiles of velocity are shown: 4 profiles are the velocity averages for intervals of data in the x; the last one is the averaged profile for all the test 1.

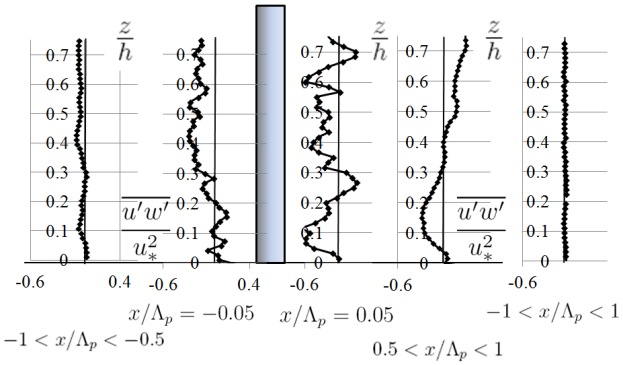

Figure 6: Profiles of averaged Reynolds stresses for different x ranges of test 1.

assume positive values. Instead, they can be positive or negative along the depth, but by averaging for all the domain (last profile in Figure 6, for $-1 < x/\Lambda_p < 1$) they assume very small values.

The behavior is totally different if, instead of test 1, is considered a section of analysis sufficiently far from the cylinder, such as in test 6 (Figures 7 and 8). It is clear that the flow becomes uniform, both from the horizontal and vertical component of velocity. Relatively to the Reynolds stresses represented in Figure 9, the first two profiles ($-1 < x/\Lambda_p < -0.5$ and $-0.5 < x/\Lambda_p < 0$) have the classical triangular trend close to the bottom. The last profile ($-1 < x/\Lambda_p < -0.5$) changes the behavior at the bottom: the Reynolds stresses go to zero, and it could be due to the effect of the wake of the closest upstream cylinder.

Finally, for quantify the changes to the averaged velocity, the averaged velocity is smaller for test closer to the cylinder: for the test 1, $\langle\sqrt{\bar{u}^2+\bar{v}^2}\rangle_1/\sqrt{\langle\bar{u}\rangle^2+\langle\bar{v}\rangle^2} = 0.8$ that is much smaller than the averaged velocity for the test 6, where the behavior is totally uniform (Figure 7), and the ratio of the velocities results $\langle\sqrt{\bar{u}^2+\bar{v}^2}\rangle_6/\sqrt{\langle\bar{u}\rangle^2+\langle\bar{v}\rangle^2} =$ 1.34. From the Figures 5, 6 and 9, it is evident that, in the case study, this spatial average, represented by the last profile of each figures, is not sufficient to describe the spatial variation of the flow characteristics, as it has been done by analyzing the different profiles.

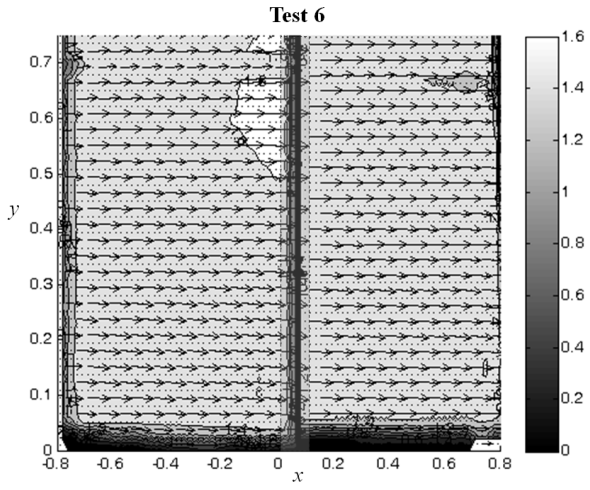

Figure 7: Time averaged velocity for the test 6. The central darkest band is caused by errors due to the superposition of the upstream and downstream images which form the global domain.

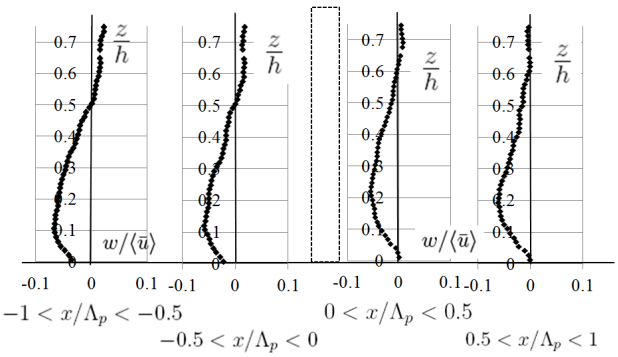

Figure 8: Vertical component of the time and spatial averaged velocity of test 6.

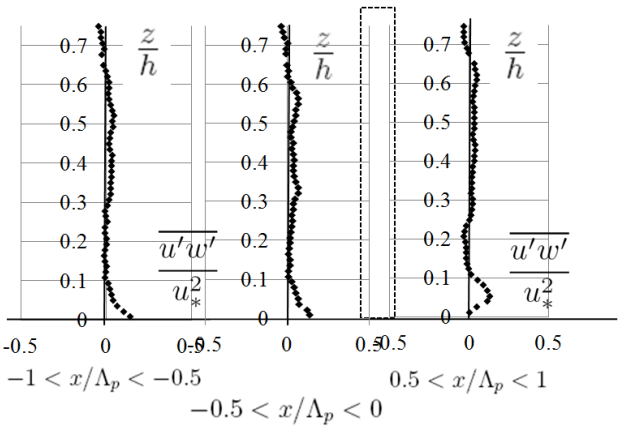

Figure 9: Averaged Reynolds stress for test 6.

Conclusion

Using the PIV technique and uniform distribution of cylinders in a laboratory channel, the parameters of classical theory of DAM are compared with local velocities. The PIV analysis has put in evidence that there is an area of the bed where the shear stress at the bottom results directed upstream, and hence where the sediments are entrained towards upstream and do not contribute to the sediment discharge, unless they reach a sufficient height to be transported by the flow. This height is as smaller as the sediment is far from the cylinder.

The results demonstrate that the double-averaged velocity is not always and completely descriptive of the behavior of the full domain of analysis, in particular if the flow field is related with the sediment transport. Whether the dispersive components would be helpful for the description of the spatial variations is an open question, that is not analyzed in the present paper.

Concluding, the mechanisms of sediment transport in vegetated rivers are different by the mechanisms of transport in unvegetated reaches, because different mechanisms of entrainment and transport have to be considered. In particular, sediment movements are not everywhere in correlation with local values of shear stress at the bottom, as usually assumed in spatially homogeneous flows. The present analysis shows that there are zones of active particle erosion but negligible transport downstream, zones of transport and zones of "sink" of sediments. All these aspects should be properly taken into account when modifications of existing sediment transport formulas or new formulation for sediment transport capacity in vegetated rivers are proposed.

References

Ettema, R., T. Nakato, and M. Muste (2008). "Estimation of scour depth at bridge abutment". In: *NCHRP Rep. No. 24* 20.

Finnigan, J. (2000). "Turbulence in plant canopies". In: *Annual Review of Fluid Mechanics* 32.1, pp. 519–571.

Ishikawa, Y., K. Mizuhara, and M. Ashida (2000a). "Drag force on multiple rows of cylinders in an open channel". In: *Grant-in-aid research project report no. 10555176*.

Ishikawa, Y., K. Mizuhara, and S. Ashida (2000b). "Effect of density of trees on drag exerted on trees in river channels". In: *Journal of Forest Research* 5.4, pp. 271–279.

Kirkil, G., SG Constantinescu, R. Ettema, et al. (2008). "Coherent structures in the flow field around a circular cylinder with scour hole". In: *Journal of Hydraulic Engineering* 134, p. 572.

Kothyari, U.C., H. Hashimoto, and K. Hayashi (2009). "Effect of tall vegetation on sediment transport by channel flows". In: *Journal of Hydraulic Research* 47.6, pp. 700–710.

Li, R.M. and H.W. Shen (1973). "Effect of tall vegetations on flow and sediment". In: *Journal of the Hydraulics Division* 99.5, pp. 793–814.

Nikora, V. (2010). "Hydrodynamics of aquatic ecosystems: an interface between ecology, biomechanics and environmental fluid mechanics". In: *River Research and Applications* 26.4, pp. 367–384.

Nikora, V. et al. (2007). "Double-averaging concept for rough-bed open-channel and overland flows: Theoretical background". In: *Journal of Hydraulic Engineering* 133, p. 873.

Righetti, M. (2008). "Flow analysis in a channel with flexible vegetation using double-averaging method". In: *Acta Geophysica* 56.3, pp. 801–823.

Righetti, M. and A. Armanini (2002). "Flow resistance in open channel flows with sparsely distributed bushes". In: *Journal of Hydrology* 269.1-2, pp. 55–64.

Tanino, Y. and H.M. Nepf (2008). "Laboratory investigation of mean drag in a random array of rigid, emergent cylinders". In: *Journal of Hydraulic Engineering* 134, p. 34.

Whitaker, S. (1999). *The method of volume averaging*. Vol. 13. Springer Netherlands.